

Local quasiparticle density of states of superconducting SmFeAsO $_{1-x}$ F $_x$ single crystals: Evidence for spin-mediated pairing

Y. Fasano^{1,[†]}, I. Maggio-Aprile¹, N.D. Zhigadlo²,

S. Katrych ², J. Karpinski² and Ø. Fischer¹

¹ *DPMC-MaNEP, University of Geneva, Switzerland and*

² *Laboratory for Solid State Physics, ETH Zurich, Switzerland*

(Dated: August 13, 2010)

Abstract

We probe the local quasiparticles density-of-states in micron-sized SmFeAsO $_{1-x}$ F $_x$ single-crystals by means of Scanning Tunnelling Spectroscopy. Spectral features resemble those of cuprates, particularly a dip-hump-like structure developed at energies larger than the gap that can be ascribed to the coupling of quasiparticles to a collective mode, quite likely a resonant spin mode. The energy of the collective mode revealed in our study decreases when the pairing strength increases. Our findings support spin-fluctuation-mediated pairing in pnictides.

PACS numbers: 74.50.+r, 74.20.Mn, 74.72.Hs

Keywords: pnictide superconductors, pairing mechanism, scanning tunnelling spectroscopy

The recent discovery of superconductivity in oxypnictides renewed the hopes on solving the longstanding puzzle of the pairing mechanism in high-temperature superconductors (HTS). This expectation is based on pnictides sharing resemblances with cuprate-HTS: superconductivity emerges when charge-doping the magnetic parent material [2], and T_c can be tuned with dopant concentration [3]. Spin-fluctuation-mediated pairing has been proposed as a promising candidate for explaining high-temperature superconductivity in oxypnictides [4–6]. In this context, electron-tunneling data can provide crucial evidence: the quantitative explanation of particular features in the electron-tunneling spectra of conventional superconductors led to unveiling their pairing mechanism [7, 8]. We use scanning tunneling microscopy (STM) to probe the local quasiparticle excitation spectrum of single-crystals of $\text{SmFeAsO}_{1-x}\text{F}_x$ [9, 10]. We detect spectral features that fingerprint the coupling of quasiparticles with a collective excitation, quite likely a spin resonant-mode [11, 12]. We find that the energy of the STM-revealed collective mode decreases when the local pairing strength increases, in remarkable similarity with the phenomenology observed in cuprates [13].

Among the similarities between pnictide and cuprate-HTS, their layered crystal structure is fundamental to compare novel electron-tunneling data in pnictides with exhaustive studies in cuprates [14]. In iron-pnictides, superconductivity is obtained by adding holes or electrons to the FePn layers (Pn: pnictogen atom) of the undoped parent compound. Depending on the number of FeAs planes per crystal unit cell (one or two), 1111 and 122-pnictides can be synthesized [10]. As in cuprates, the electronic structure of pnictides is quasi-two-dimensional [15]. Increasing the list of resemblances, a resonant magnetic excitation localized in energy and wave-vector has been detected within the superconducting phase of 122 [11] and very recently in 1111-pnictides [12]. These last two findings suggest that information on the pnictides' pairing mechanism can be obtained by analyzing electron-tunneling data with a model [16] that considers the coupling of quasiparticles with a collective mode as done in cuprates [14, 17, 18]. However, still-open issues render such a quantitative analysis not straightforward in pnictides. Undoped pnictide compounds present spin-density-wave metallic order [3] in contrast to the antiferromagnetic insulator cuprate parent compounds, making of crucial importance to study the doping-evolution of the energy of collective modes in different pnictides. In addition, the momentum structure of the superconducting gap is still subject of debate [5, 6, 19, 20]. Other issue rendering this analysis more complicated for pnictides is its multiband superconductivity [21] with up to five FeAs-related bands

crossing the Fermi level [6]. Nevertheless, an important question so far not addressed is the manifestation of collective modes that couple with quasiparticles in the excitation spectrum of pnictides.

Here we present the first STM data in single-crystals of a 1111-pnictide, nearly-optimally-doped $\text{SmFeAsO}_{1-x}\text{F}_x$ samples with nominal composition $x = 0.2$ and $T_c = 45$ K [22]. The studied crystals were grown by means of a high-pressure technique and present high structural, magnetic and transport quality as quantitatively reported in Ref. 10 We reveal spectral features that fingerprint the interaction of quasiparticles with a collective mode. We report on the pairing-strength-dependence of the mode energy, of fundamental importance on unveiling the pairing mechanism. In addition, fits of the low-bias tunneling conductance lead us to suggest that the momentum structure of the superconducting gap quite likely presents nodes. We probe the pnictides' quasiparticle excitation spectrum by mapping the local tunnel conductance dI/dV versus V_{bias} , the tip-sample voltage difference. The hundred-micron-sized crystals shown in Fig. 1 was studied using a home-made low-temperature and ultra-high-vacuum STM. Reproducible topographic images of as-grown surfaces reveal growth-terraces with terrace-valley height-differences of 1 or 2 c -axis unit cells, $c = 8.47$ Å.

Maps of local $dI/dV(V_{bias})$ spectra acquired at 4.2 K in nanometer-sized fields-of-view reveal systematic features in the quasiparticle excitation spectra whose spectral shape and energy-location spatially varies. As illustrated in Fig. 1(c), spectra are asymmetric for occupied and empty sample states. Three spectral features are systematically detected for $T < T_c$: a low-bias dI/dV depletion flanked by conductance peaks that at some locations faint on kinks (black arrows), a dip in conductance at $E_{dip} \sim 10$ meV (green circles), and a high-bias peak/kink structure at $E_2 \sim 20$ mV (green arrows). Figure 1 (d) shows the low-bias depletion fills in on warming through T_c , indicating it is the manifestation of a superconducting gap Δ . Following common practice [14], we estimate the gap as half the peak-to-peak energy separation, Δ_p . The local Δ_p values roughly follows a gaussian distribution with a mean $\langle \Delta_p \rangle = 7$ meV and a full-width at half-maximum of $\sim 0.14\langle \Delta_p \rangle$, smaller than for cuprates [14]. Point-contact spectroscopy studies in single and polycrystalline samples of $\text{SmFeAsO}_{1-x}\text{F}_x$ found similar gap values [10, 23–25], yielding $2\Delta/k_B T_c \sim 3.6$ as in classical superconductors. This ratio contrasts with roughly two-times larger values found in STM studies of 122-pnictides [26, 27], interpreted as an indication of unconventional

superconductivity in these materials.

STM measures the spectral function integrated along the pockets of the Fermi-surface and therefore lacks direct information on the k -dependence of the superconducting order parameter. However, evidence on the momentum-structure and eventual nodes of Δ can be obtained by fitting the low-bias dI/dV . This issue is related to the momentum-location of collective modes: a spin resonance located at (π, π) , as recently detected in 1111-pnictides [12], implies that the sign of Δ changes for pockets' points connected by a (π, π) vector [20, 28]. Therefore, we considered two pairing symmetries that are compatible with this scenario: sign-reversing- $s\pm$ [20] and nodal- d . For the sign-reversing- $s\pm$ symmetry Δ changes sign between the hole (α bands) and the electron (β bands) pockets whereas for the nodal- d symmetry Δ changes sign within a given pocket. The fits of the normalized tunnel conductance consider a superconducting and a normal-conducting channel amounting to circa 75% of the total conductance. The fits of the superconducting channel are based on a BCS quasiparticle excitation spectrum broadened with a finite quasiparticles' lifetime parameter and integrated along a single circular hole-pocket centered around the $(0,0)$ point. The fitting parameters are the superconducting gap Δ and the quasiparticles' lifetime $\tau = \hbar/\Gamma$ with Γ the Dynes scattering rate. Figure 2 shows the fits of average spectra with different Δ_p . For both models, the fits are robust and of similar quality: the standard deviation of the two fitted parameters is of the order of 5% for Δ and 10% for Γ for the three average spectra. The Δ and Γ values obtained for the two models are listed in the caption of Fig. 2. The Δ values obtained with the the sign-reversing- $s\pm$ fits yield $2\Delta/k_B T_c \sim 2.2$, a value too small in order to account for the T_c of the samples. In addition, the sign-reversing- $s\pm$ fits yield a significant shortening of quasiparticles' lifetime (see caption of Fig. 2). On the contrary, in the case of the nodal- d symmetry the ratio $2\Delta/k_B T_c \sim 3$ is closer to the 3.5 value that holds in most classical superconductors. These results suggest nodal- d as the most plausible candidate for the symmetry of the order parameter in $\text{SmFeAsO}_{1-x}\text{F}_x$.

We now consider the phenomenology of the spectral feature detected at E_2 . Figure 3 shows two archetypical local dI/dV curves: a hump-like structure is detected either as a kink or as a peak. Statistics on individual spectra reveal that E_2 has a larger spatial variation (full-width at half-maximum $\sim 40\%$ of the mean value) than Δ_p , see Fig. 3. In contrast with the particle-hole symmetry observed for Δ_p , the center of mass of the E_2 distributions for empty and occupied sample states are shifted by 3 meV. A similar behavior

was reported for a conductance-shoulder observed at ~ 16 meV in point-contact experiments in $\text{SmFeAsO}_{1-x}\text{F}_x$ single-crystals from the same source than ours [10]. Recent penetration depth measurements in crystals from the same batch suggest a two-gap scenario: one with magnitude in agreement with our STM data and a smaller of roughly 4 meV [29]. This evidence from bulk measurements, and the locally-observed particle-hole asymmetry of E_2 , casts doubts on the interpretation of this feature as the fingerprint of a second superconducting gap.

Alternatively, the hump-like structure can have origin in a redistribution of spectral weight as a consequence of a conductance-dip developing at energies E_{dip} , see Fig. 3 (a). In analogy to conventional and cuprate superconductors, this feature can be interpreted as a manifestation of the coupling of quasiparticles with a collective excitation [7, 8, 16–18]. Two possible candidates for the collective excitation are phonon and spin modes. Conventional electron-phonon mediated pairing in pnictides is not likely: theoretical calculations for 1111-compounds report the electron-phonon coupling is too weak to explain the materials high T_c [30], a conclusion also supported by neutron data [31]. On the other hand, a resonant spin excitation has been detected in the superconducting state of 1111 [12] and 122-pnictides [11]. Electron-tunneling data can provide information on the energy of the mode that couples with quasiparticles leading to ascertain which of the two candidates is relevant for pairing.

Indeed, the quantitative explanation of particular features in the electron-tunneling spectra of classical superconductors stand among the most convincing validations of the conventional BCS phonon-mediated pairing theory [7, 8]. In the case of cuprates, we have recently reported [17, 18] that: 1) the dip feature is the fingerprint of quasiparticles coupling with an energy and momentum-localized collective excitation, 2) the energy of the collective mode can be directly read out from dI/dV curves as $\Omega = |E_{dip} - \Delta_p|$, with 1 meV uncertainty. Here we will follow the same approach: profiting from the spatial inhomogeneity of Δ_p we study the evolution of Ω with the pairing strength. Figure 4 shows that the dip shifts towards the coherence peak when Δ_p increases, implying that the energy of the collective mode that couples with quasiparticles is anticorrelated with the local pairing strength. This result bears remarkable similarity with the phenomenology reported in the case of cuprates [13].

The value of the local collective mode energy shown in Fig. 4 ranges between 8 and 2 meV. The typical energy of the spin resonance detected by neutrons in $\text{LaFeAsO}_{1-x}\text{F}_x$,

the few available data in 1111-pnictides, is of the order of 11 meV [12]. This value is quite sensitive to the compound and the doping level, making of great importance to obtain neutron data in the particular material studied here. Nevertheless, an important result of Ref.[12] is that the spin resonance is only detected for superconducting samples. On the contrary, phonon modes are detected in parent and doped compounds, with their energy not significantly changing with temperature [31]. These findings suggest that the collective mode revealed through our analysis of STM data is quite likely the ubiquitous (π, π) spin resonant mode, signposting towards spin-fluctuation-mediated pairing in pnictides.

-
- [[†]] Present address: Instituto Balseiro and Centro Atómico Bariloche, CNEA, Argentina.
- [2] C. de la Cruz *et al.*, Nature **453**, 899 (2008).
- [3] H. Luetkens *et al.*, Nature Materials **8**, 305 (2009) .
- [4] F. Wang *et al.*, Phys. Rev. Lett. **102**, 047005 (2009).
- [5] I. I. Mazin, D. J. Singh, M. D. Johannes, and M. H. Du, Phys. Rev. Lett. **101**, 057003 (2008).
- [6] K. Kuroki *et al.*, Phys. Rev. Lett. **101**, 087004 (2008).
- [7] Giaever, I., Hart, Jr., H.R., and Megerle, K. Phys. Rev. **126**, 941 (1962).
- [8] W.L. McMillan, and J. M. Rowell, Phys. Rev. Lett. **14**, 108 (1965).
- [9] N. D. Zhigadlo, *et al.*, J. Phys.: Condens Matter, **20**, 342202 (2009).
- [10] J. Karpinski *et al.*, Physica C, **469**, 370 (2009).
- [11] A.D. Christianson *et al.*, Nature **456**, 930 (2008).
- [12] S. Wakimoto *et al.*, cond-matt:0906.2453v1 (2009).
- [13] Eschrig, M. Adv. in Physics **55**, 47-183 (2006).
- [14] Ø. Fischer *et al.*, Rev. Mod. Phys. **79**, 353 (2007).
- [15] D. J. Singh, and M.-H. Du, Phys. Rev. Lett. **100**, 237003 (2008).
- [16] M. Eschrig, and M. R. Norman, Phys. Rev. Lett. **85**, 3261 (2000).
- [17] G. Levy de Castro *et al.*, Phys. Rev. Lett. **101**, 267004 (2009).
- [18] N. Jenkins *et al.*, Phys. Rev. Lett. **103**, 227001 (2009).
- [19] A. V. Chubukov, D. V. Efremov, and I. Eremin, Phys. Rev. B **78**, 134512 (2008).
- [20] T. A. Maier, S. Graser, D. J. Scalapino, and P. Hirschfeld, Phys. Rev. B **79**, 134520 (2009).

- [21] *H. Ding et al.*, Europhys. Lett. **83**, 47001 (2009).
- [22] *S. Weyeneth et al.*, J. Supercond. Nov. Magn. **22**, 325 (2009).
- [23] *T. Y. Chen, Z. Tesanovic, R. H. Liu, X. H. Chen, and C. L. Chien*, Nature **453**, 1224 (2009).
- [24] *K. A. Yates et al.*, Supercond. Sci. Technol. **21**, 092003 (2008).
- [25] *P. Samuely et al.*, Supercond. Sci. Technol. **22**, 014003 (2009).
- [26] *Yi Yin et al.*, Phys. Rev. Lett. **102**, 097002 (2009).
- [27] *F. Massee et al.*, Phys. Rev. B **78**, 140509 (2008).
- [28] *M. M. Korshunov, and I. Eremin*, Phys. Rev. B **78**, 140509 (2008).
- [29] *L. Malone et al.*, Phys. Rev. B **79**, 140501 (2009).
- [30] *L. Boeri, O. V. Dolgov, and A. A. Golubov*, Phys. Rev. Lett. **101**, 026403 (2008).
- [31] *A.D. Christianson et al.*, Phys. Rev. Lett. **101**, 157004 (2008).

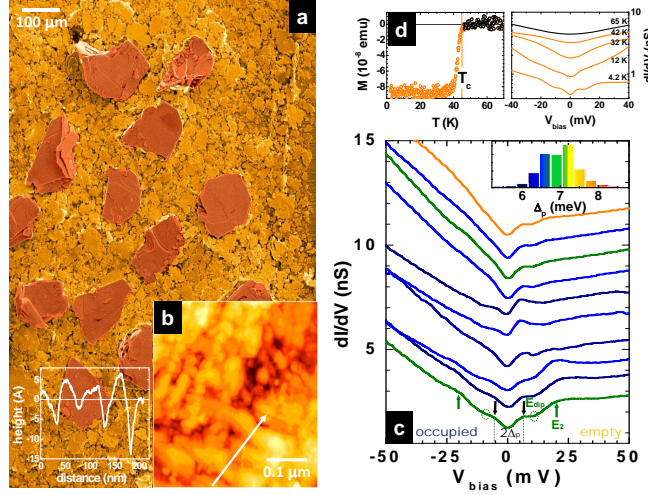


Figure 1, Fasano et al.

FIG. 1: (a) SEM image of the measured single-crystals from the same batch. (b) Right panel: STM topographic image of an as-grown surface depicting growth-terraces with a rms roughness smaller than 0.1 nm. Left panel: Height profile along the path indicated with an arrow: terrace-valley height differences are either one or two crystal unit-cell parameters ($c = 8.47 \text{ \AA}$). (c) Local dI/dV spectra (vertically shifted) acquired at 4.2 K along an 8 nm path. Spectra are color-coded according to its experimental gap value calculated as half the peak-to-peak/kink (black arrows) energy separation. The color-convention is that of the local Δ_p histogram of the insert resulting from 4500 local spectra mapped in a $40 \times 40 \text{ nm}^2$ field-of-view. Green arrows indicate the high-bias kink located at E_2 and green circles the local dip at E_{dip} . (d) Left panel: Zero-field-cooled magnetic moment of a crystal yielding $T_c = 45 \text{ K}$ and a transition width of 5 K [22]. Right panel: temperature-evolution of average dI/dV curves (in a $40 \times 40 \text{ nm}^2$ field-of-view). In the STM measurements an electrochemically-etched Ir tip served as the ground electrode and thus negative (positive) bias refers to occupied (empty) sample states. The tunnel-junction regulation parameters were of 80 meV and 1 nA. Spectra were acquired by means of a lock-in technique [14] with a bias modulation of 1.5 mV_{rms} and an energy resolution of 0.6 mV.

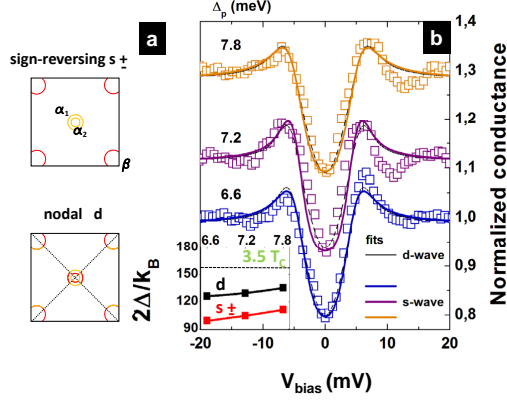


Figure 2, Fasano et al.

FIG. 2: (a) Schematics of the 1111-pnictides Fermi surface pockets (α -hole and β -electron sheets) including information on possible scenarios for the momentum-structure of the gap. The orange (red) locations represent a positive (negative) gap. Upper panel: sign-reversing $s \pm$ symmetry. Lower panel: nodal d symmetry with the dotted lines depicting the location of the gap nodes. (b) Average normalized spectra at 4.2 K obtained from hundreds of local dI/dV curves with same Δ_p (open symbols). Full lines are fits considering the sign-reversing $s \pm$ (orange, purple, blue) and nodal d (black) symmetries. A 4.2 K thermal broadening and a finite quasiparticles lifetime $\tau = \hbar/\Gamma$, with Γ the scattering rate, were considered. Sign-reversing $s \pm$ fits yield Δ 4.2, 4.3 and 4.8 meV for the average spectra with increasing Δ_p . In the case of nodal- d fits the fitted Δ values are of 5.1, 5.2, and 5.8 meV, respectively. On increasing Δ_p the scattering rate obtained in the sign-reversing- $s \pm$ fits are 0.9, 0.7 and 1.5 meV roughly twice the values obtained in the nodal- d fits, 0.3, 0.3, and 0.9 meV, respectively. Insert: Evolution of $2\Delta/k_B$ with Δ_p for the two models. The dotted line indicates the weak-coupling BCS limit of $3.5T_c$ holding for classical superconductors.

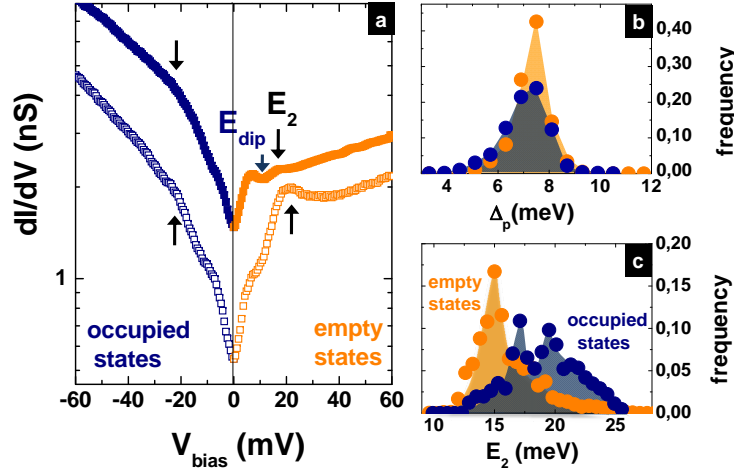


Figure 3, Fasano et al.

FIG. 3: (a) Two archetypical local dI/dV curves (vertically shifted) illustrating the spectral shape of the high-energy feature detected at E_2 (black arrows) and of the dip-like feature observed at E_{dip} (blue arrow). (b) Histograms of the energy-location of the coherence peaks/kinks, Δ_p , for empty (orange) and occupied (blue) sample states. (c) Histogram of the local E_2 values: the distribution for the empty and occupied-sample states have mean values displaced in ~ 3 meV. Histograms obtained from 4500 spectra acquired over a $40 \times 40 \text{ nm}^2$ field-of-view.

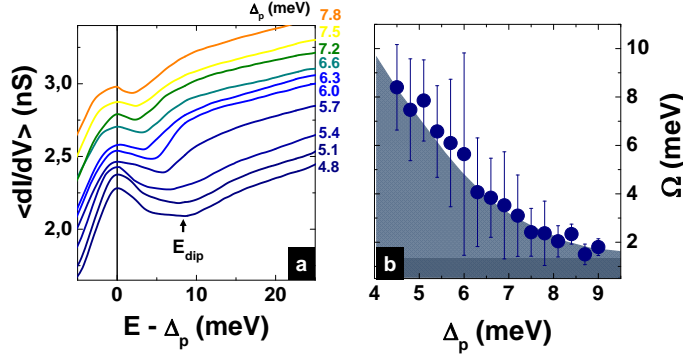


Figure 4, Fasano et al.

FIG. 4: (a) Average dI/dV curves for local spectra with the same Δ_p plotted as a function of the sample bias minus Δ_p (for the empty sample states). On increasing Δ_p the dip located at E_{dip} shifts towards the coherence peak. (b) Δ_p -dependence of the collective-mode energy measured as the peak-to-dip energy separation, $\Omega = E_{dip} - \Delta_p$. The darker region indicates the 1 meV uncertainty in determining Ω .